nature
structural &
molecular biology

A unique E1-E2 interaction required for optimal conjugation of the ubiquitin-like protein NEDD8

Danny T Huang[1,2], David W Miller[1,2], Rose Mathew[2], Robert Cassell[3], James M Holton[4], Martine F Roussel[2] & Brenda A Schulman[1,2]

Ubiquitin-like proteins (UBLs) such as NEDD8 are transferred to their targets by distinct, parallel, multienzyme cascades that involve the sequential action of E1, E2 and E3 enzymes. How do enzymes within a particular UBL conjugation cascade interact with each other? We report here that the unique N-terminal sequence of NEDD8's E2, Ubc12, selectively recruits NEDD8's E1 to promote thioester formation between Ubc12 and NEDD8. A peptide corresponding to Ubc12's N terminus (Ubc12N26) specifically binds and inhibits NEDD8's E1, the heterodimeric APPBP1–UBA3 complex. The structure of APPBP1–UBA3–Ubc12N26 reveals conserved Ubc12 residues docking in a groove generated by loops conserved in UBA3s but not other E1s. These data explain why the Ubc12-UBA3 interaction is unique to the NEDD8 pathway. These studies define a novel mechanism for E1-E2 interaction and show how enzymes within a particular UBL conjugation cascade can be tethered together by unique protein-protein interactions emanating from their common structural scaffolds.

Over a dozen UBLs in higher eukaryotes function by covalently modifying myriad substrates[1]. The best-understood functional consequence of UBL modification is ubiquitin-mediated proteolysis. However, different UBLs alter the functions of their targets in different ways, for example by changing the target's subcellular localization, enzymatic activity or protein-protein interactions. Ubiquitin's closest relative, NEDD8, does not direct its targets to the proteasome. Rather, NEDD8 is conjugated to the cullin subunits of SCF (Skp1-cullin-F-box) and related ubiquitin ligases to alter their activity[2–4]. NEDD8 enhances the ability of SCF to multiubiquitinate substrates, and displaces the CAND1 inhibitor of SCF assembly[5–8]. The NEDD8 pathway is essential in organisms ranging from fission yeast to mammals[9,10], and regulates many important biological processes, including cell division[2,3,11], signal transduction[5] and development[12].

It is important to understand how the different UBLs are ligated to their correct targets. Different UBLs are ligated to their targets by parallel but distinct cascades of enzymes that sequentially involve an E1 activating enzyme, an E2 conjugating enzyme and an E3 ligase[13,14]. First, the E1 binds the UBL, Mg^{2+} and ATP and catalyzes adenylation of the UBL's C terminus. The E1 then forms a thioester intermediate between its catalytic cysteine and the UBL's activated C terminus, and subsequently transfers the thioester-linked UBL to the catalytic cysteine of the E2 enzyme. The E3 recruits the target and facilitates UBL transfer from the E2 to a primary amino group, often from a lysine side chain, on the target.

In recent years, several general principles have emerged for protein-protein interactions in UBL transfer cascades[15–26]. Nonetheless, the selective coordination of enzymes within a particular UBL's cascade remains incompletely understood. Particularly lacking is knowledge of unique protein-protein interactions distinct for the cascades for different UBLs. The NEDD8 pathway has served as a good model for studying UBL-specific protein-protein interaction[26,51]. Although the enzymes in the NEDD8 pathway are related to those in other UBL transfer cascades, the NEDD8 pathway involves one E1, one E2 and a few E3s[3,4,27]. Moreover, it seems that NEDD8 is ultimately directed to a small number of targets[2–4]. By contrast, the ubiquitin pathway involves tens of E2s, hundreds of E3s and thousands of targets. Thus, the relatively minimal nature of the NEDD8 pathway simplifies the identification of protein-protein interactions specific for a particular UBL's conjugation cascade.

NEDD8's E2, Ubc12, has a 26-residue N-terminal extension upstream of its ~150-residue conserved E2 core domain. Ubc12's N-terminal extension is unique to the NEDD8 pathway: Ubc12's N-terminal sequence is conserved across species, but is not found in other E2s. The function of Ubc12's N-terminal extension has remained unknown. In this study we found a role for Ubc12's N-terminal extension in cell proliferation: wild-type Ubc12, but not a mutant lacking the N-terminal extension, rescues CSF-1-dependent proliferation of NIH 3T3 cells expressing a mitogenically defective but survival-competent human CSF-1 receptor. Biochemical and X-ray crystallographic studies collectively show that Ubc12's N-terminal extension is a selective peptide motif that optimally recruits NEDD8's E1 for the NEDD8 transfer cascade.

[1]Department of Structural Biology, [2]Department of Genetics and Tumor Cell Biology and [3]Hartwell Center for Biotechnology and Bioinformatics, St. Jude Children's Research Hospital, Memphis, Tennessee 38105, USA. [4]Physical Biosciences Division, Lawrence Berkeley National Laboratory, University of California, Berkeley, California 94720, USA. Correspondence should be addressed to B.A.S. (brenda.schulman@stjude.org).

Published online 5 September 2004; doi:10.1038/nsmb826

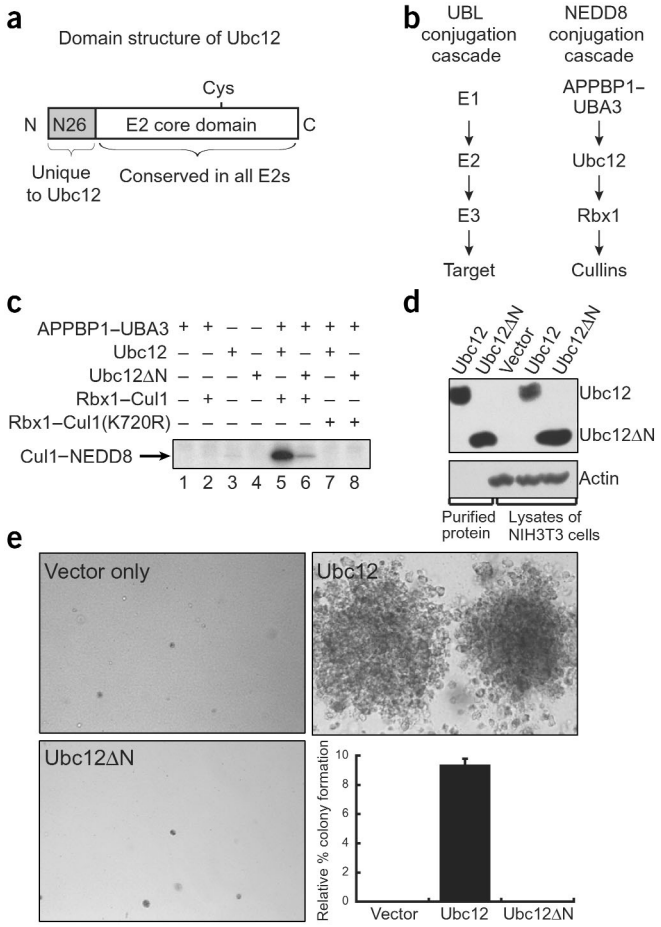

Figure 1 Ubc12's N-terminal extension is important for function. (**a**) Ubc12 has a unique 26-residue N-terminal extension conserved in Ubc12s across species but not found in other E2s. Following this sequence is the ~150-residue E2 core, which is conserved in all E2s. The position of Ubc12's catalytic Cys is shown. (**b**) NEDD8 conjugation involves the sequential action of NEDD8's E1, the heterodimeric APPBP1–UBA3 complex, NEDD8's E2, Ubc12, a RING E3 Rbx1, and cullin targets[2–4,27]. (**c**) NEDD8 conjugation to Cul1 was assayed by incubation with purified APPBP1–UBA3 (E1), Ubc12 or Ubc12ΔN lacking residues 2–26 (E2), Rbx1–Cul1 (E3-target complex, lanes 2, 5 and 6) or Rbx1–Cul1 K720R (target complex mutated at NEDD8 modification site, lanes 7 and 8) as indicated. Lanes 1–4 are controls, lane 5 shows the complete reaction with wild-type Ubc12 and lane 6 shows the reaction with Ubc12ΔN. Lanes 7 and 8 show that neither Ubc12 nor Ubc12ΔN modify Cul1 with the K720R mutation. (**d**) Immunoblot control for expression of Ubc12 and Ubc12ΔN in cell proliferation assay. (**e**) Soft agar colony formation assay of NIH 3T3 cells expressing the mutant human CSF-1R Y809F infected with retroviruses empty (top left) or expressing wild-type Ubc12 (top right) or the Ubc12ΔN mutant (bottom left) in the presence of human CSF-1. Relative percent colony formation is based on controls expressing wild-type human CSF-1R as a reference for 100% (graph, bottom right).

RESULTS

Ubc12's N-terminal extension is important for function

The sequence of Ubc12 has two regions: (i) a unique 26-residue N-terminal extension found only in Ubc12 family members and (ii) an E2 core domain, a ~150-residue domain conserved among all E2s, which contains the E2 catalytic cysteine (**Fig. 1a**). To assess whether Ubc12's N-terminal extension has any functional importance, we tested the function of a deletion mutant lacking residues 2–26, termed Ubc12ΔN, using a biochemical assay for NEDD8 transfer. The ultimate targets of NEDD8 modification include cullin family members[2–4] such as human Cul1. Cul1 is modified by NEDD8 at a single lysine, Lys720 (ref. 27). The NEDD8 transfer cascade can be reconstituted *in vitro* with the APPBP1–UBA3 heterodimeric E1 complex, the E2 Ubc12, the E3 Rbx1, the target Cul1, NEDD8, Mg^{2+} and ATP[27] (**Fig. 1b**). We monitored NEDD8 transfer using ^{32}P-labeled NEDD8 phosphorylated at an N-terminal protein kinase A site with [γ-^{32}P]ATP[28]. We found that deleting Ubc12's N-terminal extension substantially hindered Ubc12's ability to transfer NEDD8 to Cul1's Lys720 (**Fig. 1c**).

We next assayed the importance of Ubc12's N-terminal extension in cell proliferation. The NEDD8 pathway enzymes play an essential role in cell proliferation in organisms ranging from fission yeast to mammals[9,10]. Consistent with this function, we identified Ubc12 in a genetic screen for proteins involved in cell proliferation (R.M and M.F.R., unpublished results). This same screen previously identified cell cycle regulatory proteins such as Myc and D-type cyclins[29,30]. Therefore, we assayed Ubc12's effects on cell proliferation as follows: ectopic expression of the human macrophage colony-stimulating factor 1 (CSF-1) receptor (CSF-1R) in NIH 3T3 mouse fibroblasts allows the cells to survive, migrate and proliferate in serum-free medium and form colonies in soft agar the presence of human CSF-1 as the sole growth factor[31]. By contrast, cells expressing CSF-1R with the Y809F mutation in the T loop survive and remain arrested in G1, but fail to proliferate and form colonies in soft agar when stimulated with the CSF-1 growth factor[29]. As with Myc and D-type cyclins[29,30], which are other regulators of mitogenesis, retroviral expression of Ubc12 in these cells allowed proliferation in soft agar in the presence of human CSF-1 (**Fig. 1d,e**). Unlike wild-type Ubc12, Ubc12ΔN did not support proliferation, even though the wild-type and mutant Ubc12 proteins were expressed at similar levels (**Fig. 1d,e**). Therefore, the N-terminal extension of Ubc12 plays an important role in mitogenesis, as well as *in vitro*.

Ubc12's N-extension interacts selectively with NEDD8's E1

We next sought to identify the biochemical basis for Ubc12ΔN's defect in NEDD8 transfer. Ubc12 is involved in multiple steps in NEDD8 transfer: (i) interaction with NEDD8's E1, the APPBP1–UBA3 complex (ii) receiving NEDD8 from APPBP1–UBA3's catalytic cysteine in a transthiolation reaction (iii) interaction with the RING E3 Rbx1, and finally (iv) conjugation of NEDD8 to Cul-1's Lys720. To identify whether Ubc12ΔN is defective at the first two steps in the reaction, we carried out kinetic analyses, monitoring the initial rate of APPBP1–UBA3-dependent transfer of ^{32}P-labeled NEDD8 onto Ubc12's catalytic cysteine, as a function of Ubc12 concentration (**Fig. 2a**). The k_{cat} values for forming the Ubc12-NEDD8 and Ubc12ΔN-NEDD8 thioester complexes were similar, suggesting that Ubc12ΔN is chemically competent for the transthiolation reaction (**Supplementary Table 1** online). However, the K_m for Ubc12ΔN (209 ± 11 nM) is ~25-fold higher than that of wild type (5,150 ± 153 nM), indicating a defect in binding to APPBP1–UBA3 (**Supplementary Table 1** online).

To test whether Ubc12ΔN is competent to transfer NEDD8 to Cul1, we examined Ubc12ΔN-mediated formation of the Cul1–NEDD8 complex in the presence of increased APPBP1–UBA3. These experiments were done at identical concentrations of NEDD8, Ubc12, Ubc12ΔN and Rbx1–Cul1, with the only difference being the concentration of the APPBP1–UBA3 E1 complex. Twenty-fold higher levels

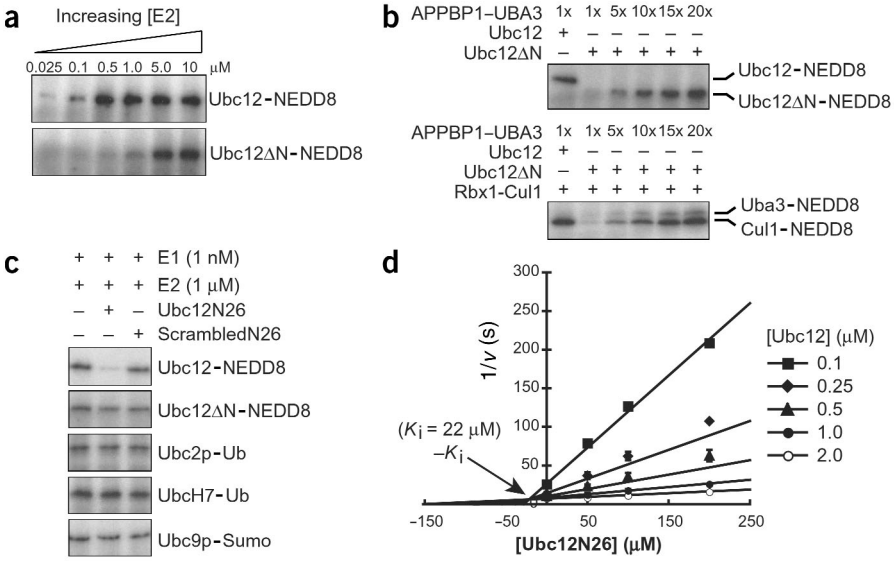

Figure 2 Ubc12's N terminus is involved in E1 binding. (**a**) Ubc12ΔN is impaired in forming a thioester complex with NEDD8. Ubc12-NEDD8 and Ubc12ΔN-NEDD8 thioester formation was examined as a function of E2 concentration. The 30 s time-point is shown for reactions involving 1 nM APPBP1–UBA3 and 25 nM, 100 nM, 500 nM, 1 μM, 5 μM and 10 μM Ubc12 or Ubc12ΔN, from left to right. (**b**) Ubc12ΔN is competent for NEDD8 conjugation to Cul1. Top, Ubc12ΔN-NEDD8 thioester formation with increasing concentrations of the APPBP1–UBA3 E1 complex. Bottom, Ubc12ΔN-mediated NEDD8 conjugation to Cul-1, with increasing concentrations of APPBP1–UBA3, assayed as in the top panel but with the addition of Rbx1–Cul1. (**c**) Ubc12N26 peptide (1 mM) corresponding to the N-terminal 26 residues of Ubc12 inhibits APPBP1–UBA3-catalyzed Ubc12-NEDD8 thioester formation, but not thioester formation between Ubc12ΔN and NEDD8, or E1 for ubiquitin–catalyzed Ubc2p-ubiquitin or UbcH7-ubiquitin thioester formation, or E1 for Sumo–catalyzed Ubc9p-Sumo thioester formation. A peptide with identical composition but scrambled sequence (ScrambledN26) had no effect. (**d**) Dixon plot analyzing inhibition of APPBP1–UBA3-catalyzed Ubc12-NEDD8 thioester formation by the Ubc12N26 peptide. The Ubc12N26 peptide is a competitive inhibitor with a K_i of 22 ± 5 μM.

of the APPBP1–UBA3 E1 complex were sufficient to allow Ubc12ΔN to form a thioester intermediate with NEDD8, and to ligate NEDD8 to Cul1 to the same degree as wild-type Ubc12 (**Fig. 2b**). These results suggest that Ubc12ΔN's primary defect in the NEDD8 pathway arises from its decreased binding to E1.

We tested direct binding to APPBP1–UBA3 with a 26-residue synthetic peptide corresponding to the sequence of Ubc12's N-terminal extension, referred to as Ubc12N26. A peptide with identical composition but scrambled sequence was used as a control (ScrambledN26). Ubc12N26 competitively inhibited formation of the Ubc12-NEDD8 thioester with a K_i of 22 μM, whereas the scrambled control peptide had no effect (**Fig. 2c,d**). The Ubc12N26 peptide had no effect on Ubc12ΔN-NEDD8 thioester formation, nor on the ability of the E1s for ubiquitin and Sumo to catalyze E2-ubiquitin and E2-Sumo thioester formation (**Fig. 2c**). In addition, deletion of Ubc12's N-terminal extension eliminated Ubc12's ability to coelute with APPBP1–UBA3 during gel filtration chromatography (data not shown). These findings suggest that Ubc12's N-terminal extension binds directly and selectively to APPBP1–UBA3.

Overall structure of the Ubc12N26 complex with NEDD8's E1

To understand how Ubc12's N-terminal extension interacts with APPBP1–UBA3, we determined the crystal structure of the APPBP1–UBA3–Ubc12N26 complex at a resolution of 2.6 Å (**Fig. 3** and **Table 1**). Structures of NEDD8's heterodimeric E1, the APPBP1–UBA3 complex, alone and in complex with NEDD8 and ATP, have been determined previously[26,28]. The previous structures reveal that the E1 contains three domains. An adenylation domain containing the ATP-binding site is linked through flexible loops to a domain organized around the catalytic cysteine, and to the C-terminal domain, which is also involved in E2 binding. The domains are organized around two clefts in the middle (**Fig. 4**). From the direction facing the catalytic cysteine, with the catalytic cysteine domain located above the adenylation domain, cleft 1 is on the left and cleft 2 is on the right (**Fig. 4**, middle panels). The large size of the two clefts suggested that they accommodated the E1's substrates[28], and the structure of the APPBP1–UBA3–NEDD8–ATP complex revealed ATP binding in cleft 1 and the globular domain of NEDD8 binding in cleft 2 (ref. 26). There are no substantial conformational changes in structure of APPBP1–UBA3 upon Ubc12N26 peptide binding (r.m.s. deviation of 0.517 Å over 917 Cα atoms between apo APPBP1–UBA3 (ref. 28) and APPBP1–UBA3–Ubc12N26).

In the APPBP1–UBA3–Ubc12N26 peptide complex, residues 1–13 of the Ubc12N26 peptide are ordered and adopt an extended structure. The Ubc12N26 peptide docks in a groove in the adenylation domain portion of UBA3 (**Fig. 4**). This portion of UBA3 has a central eight-stranded mixed β-sheet (strands a–d and g–j). In the previous APPBP1–UBA3–NEDD8–ATP structure, ATP and NEDD8 bind

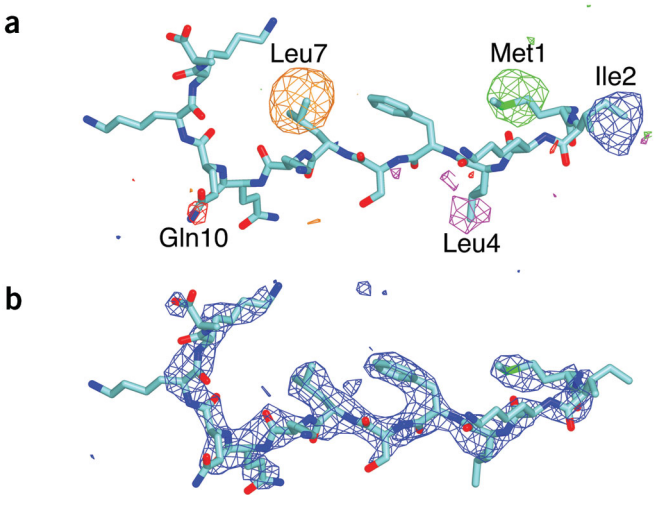

Figure 3 Electron density maps superimposed with the Ubc12N26 peptide structure. (**a**) SeMet scanning of Ubc12N26. Overlay of five different selenium anomalous difference Fourier maps contoured at 3.2 σ, obtained from crystals containing Ubc12N26 peptides with each of the following residues substituted one at a time with SeMet: Met1 (green map), Ile2 (blue map), Leu4 (magenta map), Leu7 (orange map), and Gln10 (red map). (**b**) $F_o - F_c$ map contoured at 3 σ calculated after simulated annealing was carried out at 4,000 K on the model lacking the Ubc12N26 peptide.

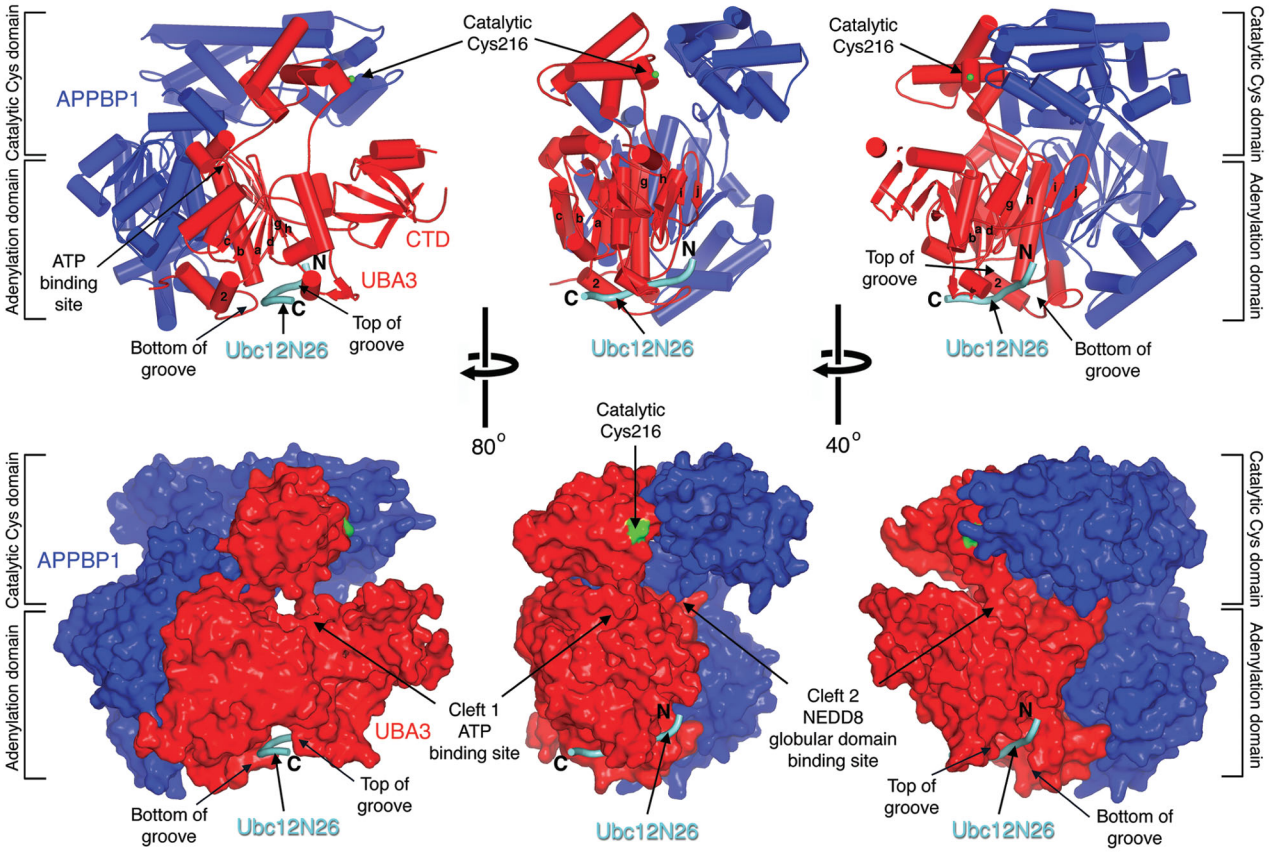

Figure 4 Overall architecture of the APPBP1–UBA3–Ubc12N26 complex. Three views of the complex are shown in cartoon (top) and surface representations (bottom), each view with a 40–80° rotation around the *y*-axis as indicated. APPBP1 is blue, UBA3 is red, Ubc12N26 is cyan, and the position of the catalytic cysteine (C216A here) is green. The locations of the adenylation domain with its ATP-binding site, the catalytic cysteine domain, the C-terminal domain (CTD) and the binding site for NEDD8's globular domain are indicated. In the middle view, cleft 1, which binds ATP, is on the left, and cleft 2, which binds the globular domain of NEDD8, is on the right. Residues 1 and 13 at the N and C termini of the visible portion of the Ubc12N26 peptide are labeled N and C, respectively. The top and bottom sides of UBA3's Ubc12N26-binding groove are labeled.

across one surface of the sheet, facing the catalytic cysteine domain. The Ubc12N26 peptide binds across the opposite face of the β-sheet. The N terminus of Ubc12 approaches the edge of the sheet nearest the binding site for NEDD8's globular domain. The observed C terminus of the peptide (Ubc12's residue 13) approaches the edge of the sheet near the ATP-binding site, and is ~55 Å from UBA3's catalytic cysteine. The peptide-binding groove is produced by the splayed-apart ends of β-strands a, d and g–j (**Fig. 4**, top left panel). The 'top' side of the peptide-binding groove comes from loops at the N termini of β-strands d and g and at the C termini of β-strands h and j. The 'bottom' side of the groove is formed by UBA3's helix 2 and the N terminus of the subsequent β-strand a, and the loop preceding β-strand i.

Structural basis for selective interactions with Ubc12N26

To understand the selectivity of Ubc12's N-terminal extension toward NEDD8's E1, we examined the conservation of the E1 docking groove in the sequences of other UBL-activating enzymes. We aligned the sequence of the Ubc12N26-binding domain of UBA3 (residues 9–205 and 288–346) with the corresponding sequences either in UBA3s from

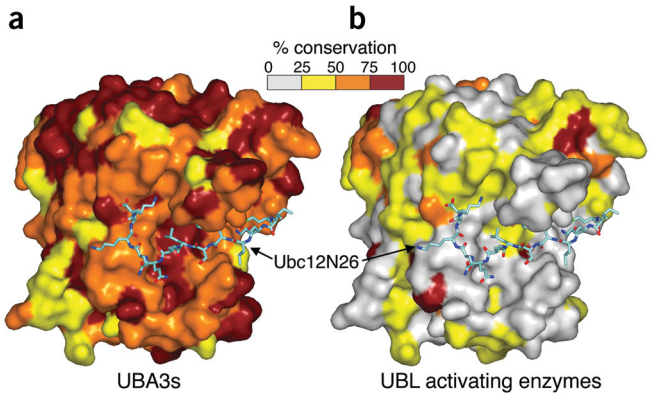

Figure 5 The Ubc12N26-binding surface is conserved in UBA3s, but not in activating enzymes for other UBLs. The structure of Ubc12's N-terminal peptide (cyan) is shown in a surface representation of the Ubc12N26-binding domain of UBA3 (residues 9–205 and 288–367), rotated ~90° about the *x*-axis relative to the middle orientation in **Figure 4**, for a direct view of the peptide contacts. (**a**) The surface is colored according to conservation among UBA3s from eight species: *Homo sapiens*, *Rattus norvegicus*, *Mus musculus*, *Arabidopsis thaliana*, *Caenorhabditis elegans*, *Drosophila melanogaster*, *Danio rerio* and *Schizosaccharomyces pombe*. (**b**) The surface is colored according to conservation among the corresponding region of activating enzymes for eight different UBLs: human NEDD8, ubiquitin, Sumo and ISG15, *S. cerevisiae* Urm1p and Apg8p, and *E. coli* MoaD and ThiS.

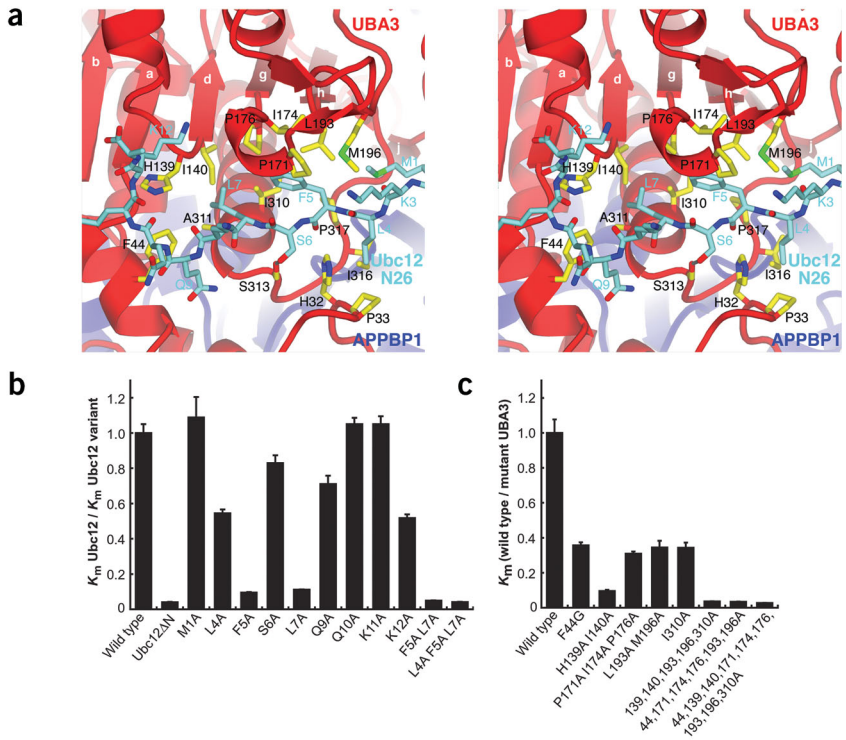

Figure 6 Contributions of individual residues from Ubc12's N-terminal peptide to E1 binding. (**a**) Stereo view of interactions between APPBP1–UBA3 and Ubc12's N-terminal peptide, with the structure rotated ~90° about the *x*-axis relative to the middle orientation in **Figure 4** for a direct view of the peptide contacts. APPBP1 is blue, UBA3 is red with side chains in yellow, and Ubc12N26 is cyan. Nitrogen, blue; oxygen, red; sulfur, green; hydrogen bonds, dashed. (**b**) Effects of alanine substitutions in Ubc12 on the relative binding affinity as a substrate for NEDD8's E1, APPBP1–UBA3, plotted as (K_m of wild-type Ubc12 / K_m of indicated variant of Ubc12). (**c**) Effects of mutations in UBA3 on the relative binding affinity for Ubc12 as a substrate plotted as K_m of Ubc12 (wild-type APPBP1–UBA3 / APPBP1-indicated variant of UBA3).

different species, or in activating enzymes for the following UBLs: human ubiquitin, Sumo and ISG15, *Escherichia coli* MoaD and ThiF, and *Saccharomyces cerevisiae* Apg8p and Urm1p. There is a high degree of conservation in the binding groove for Ubc12's N-terminal extension among UBA3 family members from different species (**Fig. 5**). However, the groove is poorly conserved among activating enzymes for different UBLs, explaining the lack of interaction we observe between the Ubc12N26 peptide and the E1s of ubiquitin and Sumo. Thus, the structure of the APPBP1–UBA3–Ubc12N26 peptide complex reveals how, within the conserved structural scaffold of an E1, unique surfaces can be generated that mediate distinct, specific protein-protein interactions.

The Ubc12N26-UBA3 interface

The extended conformation of the Ubc12N26 peptide is stabilized by numerous hydrogen bonds between UBA3 and the peptide backbone, burying 950 Å^2 of the Ubc12N26 peptide's surface area. The complex is anchored by burial of two hydrophobic residues from Ubc12, Phe5 and Leu7, in a broad cavity on the top side of the groove (**Fig. 6a**). In contrast to the Ubc12 portion of this interaction, which is dominated by only two hydrophobic side chains, the UBA3 portion of this interaction involves numerous residues. UBA3's Phe44, Cys49, His139, Ile140, Pro171, Ile174, Pro176, Leu193, Met196, Ile310, Ala311 and Pro317 line the broad cavity that interacts with Ubc12N26's Phe5 and Leu7. Facing the opposite, bottom side of the groove, Ubc12's Leu4 makes hydrophobic contacts with UBA3's His32, Pro33 and Ile316, and Ubc12's Ser6 forms a hydrogen bond with UBA3's Ser313. The observed portion of the peptide sequence is anchored at both ends, with Ubc12's N-terminal Met1 tucking into one end of UBA3's broad hydrophobic cavity, and Lys12's side chain forming hydrogen bonds with the carbonyls from UBA3's Arg136 and Phe138.

The roles of individual residues in Ubc12's N-terminal extension were assessed by testing the effects of single alanine substitutions on Ubc12-NEDD8 thioester formation. Mutations of Phe5 and Leu7 have the greatest effect (**Fig. 6b** and **Supplementary Table 1** online), indicating that the burial of these hydrophobic side chains contributes the bulk of the binding energy. Smaller effects result from mutating Leu4

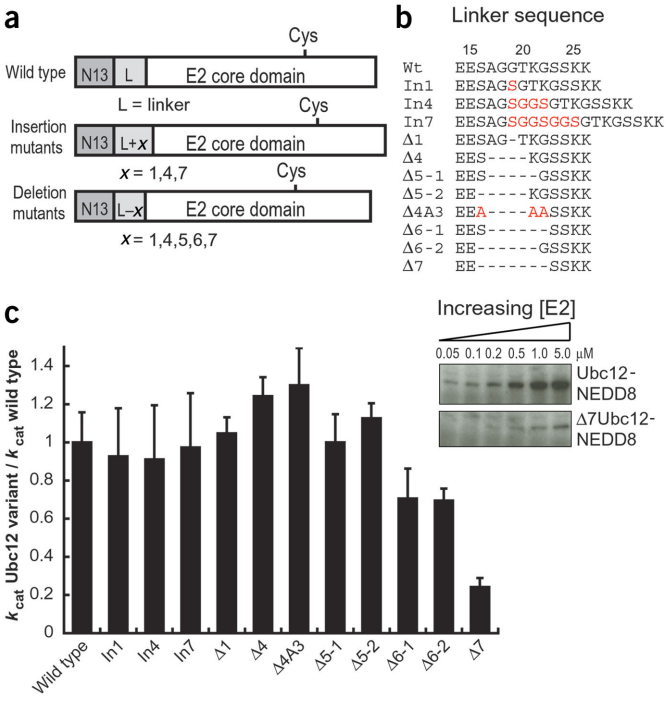

Figure 7 Minimal length requirement for the linker between the E1 docking motif and the E2 core domain in Ubc12. (**a**) Schematic diagram of insertion and deletion mutants used for these experiments. (**b**) Sequences of Ubc12 linkers (residues 14–26 in wild-type Ubc12) for insertion and deletion mutants used for these experiments. Insertions and amino acid changes are red, and deletions are denoted by dashes. (**c**) k_{cat} Ubc12 variant / k_{cat} wild-type Ubc12 for the one-, four- and seven-residue insertion mutants (In1, In4 and In7), the one-, four-, five-, six- and seven-residue deletion mutants (Δ1, Δ4, Δ5-1, Δ5-2, Δ6-1, Δ6-2 and Δ7) and an additional alanine-containing mutant to control for sequence requirements (Δ4A3), as indicated. Inset, Ubc12-NEDD8 thioester formation for wild-type Ubc12 and the seven-residue deletion mutant, Δ7.

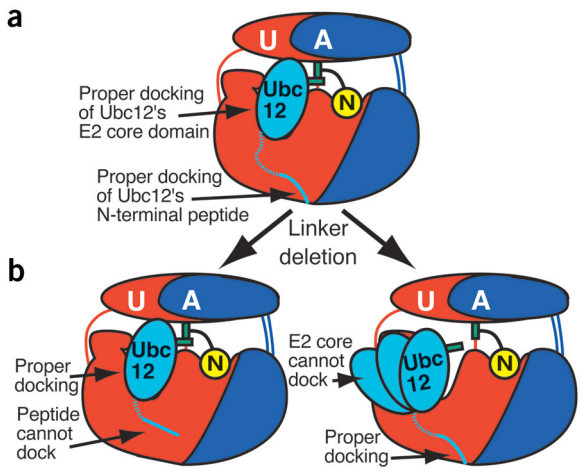

Figure 8 Model for optimal positioning of Ubc12 in the E1 structure for formation of the Ubc12-NEDD8 thioester. APPBP1 is blue, UBA3 is red, NEDD8 is yellow, Ubc12 is cyan, and catalytic cysteines are green. (**a**) Ubc12's interaction with APPBP1–UBA3 is bipartite: both Ubc12's N-terminal peptide and conserved E2 core domain must bind the E1 simultaneously for optimal Ubc12-NEDD8 thioester formation. (**b**) Deletions of six or more residues from the linker between Ubc12's N-terminal docking peptide and E2 core domain are deleterious, either preventing docking of the N-terminal docking sequence (left) or the E2 core domain (right). The minimum length of 8 residues between Ubc12's N-terminal 13-residue docking peptide and E2 core domain suggests that the E2 core domain binds cleft 1 in the APPBP1–UBA3 structure.

and Lys12. The F5A L7A double mutation results in a ~20-fold increase in K_m, and the triple mutant, which also contains a L4A substitution, has the same effect on K_m as deleting the entire 26-residue N-terminal extension (**Fig. 6b** and **Supplementary Table 1** online). Leu4, Phe5 and Leu7 are conserved as hydrophobic residues among Ubc12 family members from different species, suggesting that their N-terminal extensions will bind their UBA3s in a similar manner.

The broad cavity from UBA3 that recognizes Ubc12's Phe5 and Leu7 involves numerous hydrophobic side chains. The roles of different parts of UBA3's cavity were tested by assaying the effects of mutating side chains from different regions of the groove (**Fig. 6c** and **Supplementary Table 1** online). All of the mutations affect the K_m for Ubc12-NEDD8 thioester formation without affecting k_{cat}. The binding affinity for Ubc12 in the transthiolation reaction further decreases as the number of mutations increases, reflecting the importance of UBA3's entire broad cavity in recognizing Ubc12's N-terminal extension.

Optimal spacing between Ubc12's N-extension and core domain

If Ubc12's N-terminal peptide and E2 core domain bind the E1 simultaneously, then there should be a minimal length requirement for the linker between the two domains of Ubc12. To address this possibility, we made deletions and insertions between Ubc12's residues 16 and 23 based on (i) the location of these residues in the sequence, between Ubc12's N-terminal residues ordered in the crystal structure (residues 1–13) and E2 core domain (Ubc12 residues 27–183); (ii) the low sequence complexity of these residues (sequence SAGGTKG); and (iii) the finding that mutating the Leu4, Phe5 and Leu7 side chains has the same effect as deleting the entire N-terminal peptide, suggesting that no other side chains contribute substantially to the binding of Ubc12's N-terminal 26 residues. Insertions of up to seven glycine and serine residues and deletions of up to five residues had little effect on the kinetics of Ubc12-NEDD8 thioester formation. Removing six residues had a small effect (**Fig. 7** and **Supplementary Table 1** online). In contrast, deleting seven residues was highly detrimental (**Fig. 7** and **Supplementary Table 1** online). To control for sequence effects, we tested the activity of a four-residue deletion with three flanking residues mutated to alanines (Δ4A3, **Fig. 7b,c**). The results indicate that there is not a requirement for the sequence removed in the seven-residue deletion (**Fig. 7** and **Supplementary Table 1** online). Therefore, the deleterious effect of the seven-residue deletion reflects a minimum length requirement between Ubc12's E1-docking peptide and E2 core domain.

In contrast to removal of the entire peptide extension, which affects only K_m, the deletion of the seven-residue linker affected both K_m and k_{cat}. This was probably caused by a combination of two effects. First, formation of the productive complex would involve Ubc12's catalytic cysteine approaching APPBP1–UBA3's catalytic cysteine (**Fig. 8a**). In the seven-residue deletion mutant, the linker between Ubc12's catalytic cysteine–containing E2 core domain and N-terminal docking sequence is too short to allow docking of the peptide in the productive complex (**Fig. 8b**, left panel). Second, docking of Ubc12's N-terminal peptide in the seven-residue deletion mutant would prevent proper docking of the E2 core domain (**Fig. 8b**, right panel). Thus, the interaction of Ubc12 with APPBP1–UBA3 is bipartite: both Ubc12's N-terminal peptide and conserved E2 core domain bind the E1 simultaneously for optimal Ubc12-NEDD8 thioester formation.

The distance between Ubc12's docking peptide and E2 core domain can be estimated based on the minimum number of linker residues required for optimal activity. With an approximation of 3.5 Å per residue for an extended conformation and a minimum requirement for eight linker residues (equivalent to the five-residue deletion), the distance is ~28 Å between the C terminus of the docking peptide and N terminus of the E2 core domain. With the additional constraint that the E1 and E2 catalytic cysteines will be in proximity in the productive complex, the most likely location for the conserved catalytic E2 core domain to bind the E1 structure is in cleft 1 (**Fig. 8**).

DISCUSSION

We find that Ubc12's unique N-terminal extension tethers Ubc12 selectively to APPBP1–UBA3 via a novel type of E1-E2 interaction. First, deletion of Ubc12's N-terminal extension reduces the K_m, but not the k_{cat}, for APPBP1–UBA3-catalyzed Ubc12-NEDD8 thioester formation. Second, a peptide corresponding to Ubc12's N-terminal 26 residues inhibits NEDD8-Ubc12 thioester formation. This effect is specific to the NEDD8 pathway, because the peptide does not affect thioester formation between ubiquitin or Sumo and their E2s (**Fig. 2c**). Third, deletion mutations reveal a minimum length requirement for the linker between Ubc12's docking peptide and E2 core domain. These results suggest that for the NEDD8 pathway, the E1-E2 interaction is bipartite: both Ubc12's docking peptide and catalytic core domain must bind the E1 simultaneously for optimal transfer of NEDD8 from E1 to E2.

The crystal structure of the APPBP1–UBA3–Ubc12N26 peptide complex reveals that Ubc12's peptide-like extension interacts with a docking groove generated from unique loop sequences in UBA3. Even though the docking peptide and docking groove sequences are unique to Ubc12 and UBA3 family members, respectively, the adenylation domain portion of UBA3 that contains the docking groove corresponds to the most conserved domain in UBL-activating enzymes[13,32]. Thus, the structure reveals how unique protein-protein interactions,

Table 1 Data collection and refinement statistics

	APPBP1–UBA3–Ubc12N26
Data collection	
Space group	$P2_12_12_1$
Cell dimensions	
a, *b*, *c* (Å)	92.4, 122.8, 195.9
α, β, γ (°)	90.0, 90.0, 90.0
Resolution limit (Å)	2.6
R_{sym}	7.0 (35.6)
$I / \sigma I$	30.4 (3.6)
Completeness (%)	99.7 (99.7)
Mean redundancy	31.8
Refinement	
Resolution (Å)	18.0–2.6
No. reflections	2,157,076
No. unique reflections	67,734
R_{work} / R_{free}	23.7 / 27.9
No. atoms	
Protein	14,344
Zinc	2
Water	298
B-factors	
Protein	68.3
Zinc	49.1
Water	56.0
R.m.s. deviations	
Bond lengths (Å)	0.008
Bond angles (°)	1.42

Values in parentheses are for the highest-resolution shell.

specific for a particular UBL's pathway, can be generated from a common structural scaffold such as an E1 adenylation domain.

Many post-translational modifications are directed to their targets via multienzyme cascades. In addition to UBL modification cascades, some of the best-studied examples of multienzyme post-translational modification cascades are serine/threonine phosphorylation pathways, such as MAP kinase (MAPK) and cyclin-dependent kinase (CDK) cascades. Several characteristics of the interaction between NEDD8's E1 and the peptide from NEDD8's E2 are reminiscent of interactions in these pathways. MAPKs and CDKs bind their targets through interactions between docking peptides and docking grooves[33,34]. Similar to APPBP1–UBA3's interactions with Ubc12, the interactions of MAPKs and CDKs with the downstream enzymes in their cascades are often bipartite, with both a docking peptide binding distal from the active site and the target's phosphoacceptor sequence binding at the kinase active site. A primary function of the docking peptide interaction with these kinases is to reduce the K_m of the target[35]. Thus, the APPBP1–UBA3–Ubc12N26 interaction reveals that common design principles underlie these very divergent multienzyme post-translational modification cascades.

The interaction between E1 and the E2's N-terminal peptide found between APPBP1–UBA3 and Ubc12 is probably unique to the NEDD8 pathway, because many E2s for other UBLs lack N-terminal extensions. We wonder why the NEDD8 cascade requires additional E1-E2 interactions. Clues to a possible function for this interaction come from the paradigm of interactions between docking grooves and docking peptides established by serine/threonine phosphorylation cascades. In MAPK or CDK cascades, the kinase docking groove is multifunctional, recruiting not only targets, but also regulatory proteins such as other kinases, phosphatases and inhibitors, which all contain similar docking peptide sequences[33,34]. For example, part of the function of some CDK inhibitors comes from their ability to displace peptide-like docking sequences in substrates[33]. Notably, a UBA3-binding protein, But1, has recently been identified in fission yeast[36]. But1's biological function is consistent with an inhibitory role in the NEDD8 pathway[36]. The But1 sequence contains many **Φ**-**Φ**-X-**Φ** (where **Φ** indicates a hydrophobic residue and X indicates any residue) sequences similar to the Leu4-Phe5-Ser6-Leu7 sequence, which we find anchors Ubc12 in UBA3's docking groove. Future studies will reveal whether But1 or other proteins bind to UBA3 via the Ubc12 docking groove to inhibit NEDD8 conjugation.

Another possible function for the additional APPBP1–UBA3–Ubc12N26 interaction comes from the marked specificity of the NEDD8 pathway[2–4]. NEDD8 modification of cullins is one of many regulatory mechanisms controlling ubiquitin conjugation by SCF and related E3s. Consistent with its important regulatory function, NEDD8 modification of cullins is controlled not only by the conjugation pathway, but also by deconjugation by the COP9 signalosome[37], underscoring the importance of precision in this pathway. The additional E1-E2 interaction may serve to ensure the selectivity of the NEDD8 conjugation cascade.

Like Ubc12, many other E2s also have their own distinct extensions at their N and C termini, beyond the conserved E2 core domain. The molecular functions of only a handful of these extensions are known[38–41], and to date, the structural basis for protein-protein interactions mediated by these extensions remains elusive. One of the best-understood extensions is in the E2 Ubc2p, which interacts with the E3 Ubr1p. Although the Ubc2p-Ubr1p interaction is likely to involve interactions common to E2–E3 complexes because it requires Ubr1p's RING domain, Ubc2p's C-terminal extension is also known to stabilize the interaction with Ubr1p[42]. Therefore, it is likely that the extensions on other E2s function in a manner analogous to Ubc12's, strengthening interactions between enzymes in other UBL modification cascades.

The importance of Ubc12's N-terminal extension is further underscored by the detrimental effect of the Ubc12ΔN deletion in our cell proliferation assay. The best-characterized targets of Ubc12 are cullins[2–12,43], although we do not yet know which targets are important in our assay. Cul1-, Cul2-, Cul3- and Cul4a-containing ubiquitin ligases are known to promote the degradation of key regulators of cell proliferation, including cyclins, CDK inhibitors, proteins involved in DNA replication, proteins involved in mitotic spindle assembly, transcription factors and proteins involved in signal transduction (reviewed in ref. 43). It will be of interest to determine which targets of Ubc12-mediated NEDD8 conjugation are involved in the CSF-1-dependent proliferation. Our finding that Ubc12ΔN is defective in this cell proliferation assay raises the possibility that APPBP1–UBA3 and Ubc12 may serve as good targets for antimitogenic agents.

METHODS

Protein and peptide preparation. All constructs were generated by standard PCR-ligation molecular biology methods. The entire coding sequence for each construct was verified by automated sequencing. All proteins were expressed as GST fusions in *E. coli* strains BL21(DE3), BL21Gold(DE3), or BL21(DE3) RIL codon-enhanced strains (Novagen and Stratagene), from either pGEX4T1 or pGEX2TK (Pharmacia). The proteins were initially purified as GST fusions by glutathione affinity chromatography, and were subsequently purified to homogeneity after thrombin cleavage using a combination of ion exchange, gel filtration and glutathione affinity chromatography[26,28,44,45]. A mutant form of APPBP1–UBA3 lacking APPBP1's loop of residues 254–258 and UBA3's N-terminal 11 residues, with UBA3's catalytic Cys216 mutated to alanine, was

used for crystallization[26]. Biochemical studies used full-length, wild-type E1s[28,44,45] or APPBP1–UBA3 mutants expressed and purified as for the wild-type E1; wild-type or mutant versions of Ubc12 (ref. 28) as indicated; and the truncated active versions of ubiquitin and the UBLs human NEDD8 and *S. cerevisiae* Sumo (Smt3p) terminating with the sequence Gly-Gly[26,28,44]. The human Rbx1–Cul1 (split) complex was obtained in soluble form from *E. coli* by simultaneously coexpressing Rbx1, Cul1's N-terminal domain (residues 1–411), and Cul1's C-terminal domain (residues 411–776 at the C terminus). The complex consists of Cul1's N- and C-terminal domains associated noncovalently with each other and with Rbx1. The split Cul1–Rbx1 complex has been shown previously to have the same three-dimensional structure and ubiquitin ligase activity as the Rbx1 complex with Cul1 expressed as a single polypeptide in insect cells[45]. The 26-residue peptide corresponding to Ubc12's N terminus, termed Ubc12N26 (sequence MIKLFSLKQQKKEEESAGGTKGSSKK), the five different selenomethoionine (SeMet)-substituted Ubc12N26 peptides, and the ScrambledN26 peptide (sequence MKFQLKEIEAGKSKLKSGTSEKGQKS) were chemically synthesized with C-terminal amide blocking groups. The peptides were purified by reverse-phase HPLC, and their identities confirmed by mass spectrometry. The lyophilized peptides were dissolved in 25 mM HEPES, 150 mM NaCl, 5 mM DTT, pH 7.5, at a concentration of 10 mM.

Biochemical assays. All biochemical assays were carried out in 10 μl in 50 mM Tris-HCl, pH 7.6, 50 mM NaCl, 10 mM $MgCl_2$, 5 mM ATP, 1 mM DTT, 0.3 U ml^{-1} inorganic pyrophosphatase, 0.3 U ml^{-1} creatine phosphatase, 5 mM creatine phosphate, 2 mg ml^{-1} ovalbumin, with 5 μM NEDD8, ubiquitin or *S. cerevisiae* Sumo (Smt3p) phosphorylated at the N-terminal PKA site (from pGEX2TK) with [γ-^{32}P]ATP[28], at 18 °C, which is the ambient room temperature for our dedicated radioactivity laboratory. Reactions were quenched with an equal volume of 2× SDS sample buffer. Reactions were carried out with 1 nM of the appropriate E1, except for the modification of Cul1 by Ubc12ΔN (**Fig. 2**), which used 1, 5, 10, 15 and 20 nM APPBP1–UBA3 as indicated, and 3 μM Rbx1–Cul1. Kinetics of E1-E2 transthiolation were determined from at least seven different Ubc12 concentrations per curve, ranging from 0 to 50 μM, with reactions stopped after 30 s (ref. 46). The Cul1 modification and peptide inhibition assays were stopped after 60 s. Proteins were resolved by SDS-PAGE, dried and visualized by autoradiography. Bands were quantified using a STORM860 phosphorimager and ImageQuant software (Molecular Dynamics). Known amounts of ^{32}P-labeled NEDD8 and [γ-^{32}P]ATP were exposed together as standards. k_{cat} and K_m for E1-E2 transthiolation were determined from Lineweaver-Burk plots. The K_i of Ubc12N26 for APPBP1–UBA3-catalyzed Ubc12-NEDD8 thioester formation was determined from five different Ubc12 concentrations (0.1–2 μM) with varying concentrations of Ubc12N26 (0–1 mM), and calculated from Dixon plots using SigmaPlot 8.0 software (SPSS).

Cell culture, antibody production and immunoblotting. NIH 3T3 mouse fibroblast lines expressing the wild-type or mutant (Y809F) human CSF-1 receptors were as described[31]. For identification of Ubc12 in the human CSF-1-dependent mitogenesis assay, cells expressing human CSF-1R Y809F were infected with a retroviral MaRX rat cDNA library provided by G. Hannon (Cold Spring Harbor Laboratory)[47]. Infected cells were plated on 100-mm plates and foci of transformed cells were recovered by cylinder cloning. Integrated proviruses were recovered by digestion of the cell's high-molecular-mass DNA with the Cre recombinase, as described[47], and Ubc12 was recovered multiple times from the soft agar clones. The protein sequences of rat and human Ubc12 are identical, so human Ubc12 and Ubc12ΔN were subcloned into the pBabepuro retroviral vector for preparing high-titer retroviruses in 293T cells. NIH 3T3 cells expressing the wild-type or Y809F mutant human CSF-1R were infected with retroviruses expressing Ubc12 or Ubc12ΔN, and cloned in soft agar 2 d after infection in the presence or absence of recombinant human CSF-1 (provided by M. Clark, Genetics Institute). Lysates were also prepared in parallel and 24 μg of each protein lysate or 50 ng of purified bacterially produced wild-type or mutant Ubc12 were separated by SDS-PAGE. Proteins were analyzed by immunoblotting, with Ubc12 detected by rabbit polyclonal antiserum raised against residues 169–180 of Ubc12 (sequence RGGYIGSTYFER, generated by Rockland Immunochemicals). Anti-actin serum (C-11, Santa Cruz Biotechnology) was used to control for loading.

Crystallization, data collection and structure determination. APPBP1(Δ254–258)–UBA3(ΔN11 C216A) and Ubc12N26 were mixed at 1:5 molar ratio, and crystals were grown at room temperature by hanging- and sitting-drop vapor diffusion by mixing the complex with an equal volume of reservoir solution containing 9.5–12.5% (v/v) PEG 10k, 0.2 M KCl, 0.1 M MES, 5 mM DTT, pH 6.5. The crystals formed with two complexes in the asymmetric unit (**Table 1**). Crystals were flash-frozen in 12.5% (v/v) PEG 10k, 0.2 M KCl, 0.1 M MES, 5 mM DTT, 20% (v/v) MPD, pH 6.5, before data collection at the SERCAT beamline at the Advanced Photon Source, at the X25 beamline at the National Synchrotron Light Source, and at the 8.3.1 beamline at the Advanced Light Source. Reflection data were indexed, integrated and scaled using HKL2000 or DENZO and SCALEPACK[48] or Elves[49]. Initial phases were obtained by molecular replacement using Elves[49] with the coordinates of apo APPBP1–UBA3 (ref. 28) as a search model, or by refining the apo APPBP1–UBA3 structure against the new data using CNS[50]. Electron density for the peptide was readily visible after preliminary refinement. Because only 13 of the 26 residues in the Ubc12N26 peptide were visible in the structure, we wished to obtain independent experimental data to verify the structure of the peptide. We grew crystals of the complex with individual SeMet substitutions in place of Met1, Ile2, Leu4, Leu7 and Gln10, collected data to better than a resolution of 3.5 Å at the peak wavelength for the incorporated selenium (~0.9796 Å), and identified the locations of the seleniums by anomalous difference Fourier analysis, with phases obtained by using the apo APPBP1–UBA3 structure[28] as a search model with Elves[49]. Each selenium is located on the assigned side chain in the native structure (**Fig. 3a**), providing experimental validation for the structure of the peptide. The final model was refined at a resolution of 2.6 Å using CNS[50], and it contains two copies of the complex. The electron density is substantially better over one copy, which contains Ubc12N26 residues 1–13, APPBP1 residues 1–253 and 259–534, UBA3 residues 12–355 and 361–384, and an additional 3 residues owing to cloning at the N terminus and 43 residues in the C-terminal domain built as polyalanine, owing to weak side chain density and lack of density for loops precluding unambiguous determination of the side chains in this region. The other copy contains Ubc12N26 residues 4–13, APPBP1 residues 7–199, 211–253 and 259–534, UBA3 residues 17–354 and 361–384, and an additional 33 residues in the C-terminal domain built as polyalanine. Side chains lacking electron density were not modeled. The final model has excellent geometry, with no Ramachandran outliers in disallowed regions. Details of refinement are given in **Table 1**.

Coordinates. Coordinates and structure factors for the APPBP1–UBA3–Ubc12N26 structure have been deposited in the Protein Data Bank (accession code 1TT5).

Note: Supplementary information is available on the Nature Structural & Molecular Biology website.

ACKNOWLEDGMENTS

We are grateful to M.S. Podgorski for initial characterization of the Ubc12ΔN mutant, to P.D. Jeffrey, N.P. Pavletich, M. Pagano, L. Hendershot, H. Walden and other members of the Schulman lab for many helpful discussions, to D.L. Minor for critical reading of the manuscript, to P.J. Murray for assistance with **Figure 8**, to C. Ross for crystallography support, to G. Hannon for the MaRX library and initial experiments with Ubc12 in cell proliferation assays, to S. Olsen and K. Rakestraw for expert DNA synthesis and sequencing, and to J. Tanamachi and staff at the 8.3.1 beamline at Advanced Light Source, M. Becker and staff at the X25 beamline at National Synchrotron Light Source, and staff at the SERCAT beamline at Advanced Photon Source for synchrotron support. This work was supported by American Lebanese Syrian Associated Charities, the US National Institutes of Health (P30CA21765 National Cancer Institute Cancer Center Core grant to St. Jude, R01GM69530 to B.A.S., P01CA071907 to M.F.R.), the Department of Defense (DAMD17-03-1-0420), a grant from Phillip and Elizabeth Gross, a Pew Scholar in Biomedical Sciences award to B.A.S., and a St. Jude Special Fellowship to D.H.

COMPETING INTERESTS STATEMENT

The authors declare that they have no competing financial interests.

Received 17 May; accepted 20 July 2004
Published online at http://www.nature.com/nsmb/

1. Schwartz, D.C. & Hochstrasser, M. A superfamily of protein tags: ubiquitin, SUMO and related modifiers. *Trends Biochem. Sci.* **28**, 321–328 (2003).
2. Lammer, D. *et al.* Modification of yeast Cdc53p by the ubiquitin-related protein rub1p affects function of the SCFCdc4 complex. *Genes Dev.* **12**, 914–926 (1998).
3. Liakopoulos, D., Doenges, G., Matuschewski, K. & Jentsch, S. A novel protein modification pathway related to the ubiquitin system. *EMBO J.* **17**, 2208–2214 (1998).
4. Osaka, F. *et al.* A new NEDD8-ligating system for cullin-4A. *Genes Dev.* **12**, 2263–2268 (1998).
5. Read, M.A. *et al.* Nedd8 modification of cul-1 activates SCF(β(TrCP))-dependent ubiquitination of IκBα. *Mol. Cell. Biol.* **20**, 2326–2333 (2000).
6. Wu, K., Chen, A. & Pan, Z.Q. Conjugation of Nedd8 to CUL1 enhances the ability of the ROC1–CUL1 complex to promote ubiquitin polymerization. *J. Biol. Chem.* **275**, 32317–32324 (2000).
7. Liu, J., Furukawa, M., Matsumoto, T. & Xiong, Y. NEDD8 modification of CUL1 dissociates p120(CAND1), an inhibitor of CUL1-SKP1 binding and SCF ligases. *Mol. Cell* **10**, 1511–1518 (2002).
8. Zheng, J. *et al.* CAND1 binds to unneddylated CUL1 and regulates the formation of SCF ubiquitin E3 ligase complex. *Mol. Cell* **10**, 1519–1526 (2002).
9. Osaka, F. *et al.* Covalent modifier NEDD8 is essential for SCF ubiquitin-ligase in fission yeast. *EMBO J.* **19**, 3475–3484 (2000).
10. Tateishi, K., Omata, M., Tanaka, K. & Chiba, T. The NEDD8 system is essential for cell cycle progression and morphogenetic pathway in mice. *J. Cell Biol.* **155**, 571–579 (2001).
11. Kurz, T. *et al.* Cytoskeletal regulation by the Nedd8 ubiquitin-like protein modification pathway. *Science* **295**, 1294–1298 (2002).
12. Pozo, J.C., Timpte, C., Tan, S., Callis, J. & Estelle, M. The ubiquitin-related protein RUB1 and auxin response in *Arabidopsis*. *Science* **280**, 1760–1763 (1998).
13. Hochstrasser, M. Evolution and function of ubiquitin-like protein-conjugation systems. *Nat. Cell Biol.* **2**, E153–E157 (2000).
14. Pickart, C.M. Mechanisms underlying ubiquitination. *Annu. Rev. Biochem.* **70**, 503–533 (2001).
15. Huang, L. *et al.* Structure of an E6AP–UbcH7 complex: insights into ubiquitination by the E2-E3 enzyme cascade. *Science* **286**, 1321–1326 (1999).
16. Johnston, S.C., Riddle, S.M., Cohen, R.E. & Hill, C.P. Structural basis for the specificity of ubiquitin C-terminal hydrolases. *EMBO J.* **18**, 3877–3887 (1999).
17. Liu, Q. *et al.* The binding interface between an E2 (UBC9) and a ubiquitin homologue (UBL1). *J. Biol. Chem.* **274**, 16979–16987 (1999).
18. Mossessova, E. & Lima, C.D. Ulp1-SUMO crystal structure and genetic analysis reveal conserved interactions and a regulatory element essential for cell growth in yeast. *Mol. Cell* **5**, 865–876 (2000).
19. Zheng, N., Wang, P., Jeffrey, P.D. & Pavletich, N.P. Structure of a c-Cbl-UbcH7 complex: RING domain function in ubiquitin-protein ligases. *Cell* **102**, 533–539 (2000).
20. Brzovic, P.S., Rajagopal, P., Hoyt, D.W., King, M.C. & Klevit, R.E. Structure of a BRCA1–BARD1 heterodimeric RING–RING complex. *Nat. Struct. Biol.* **8**, 833–837 (2001).
21. Hamilton, K.S. *et al.* Structure of a conjugating enzyme-ubiquitin thiolester intermediate reveals a novel role for the ubiquitin tail. *Structure* **9**, 897–904 (2001).
22. Bernier-Villamor, V., Sampson, D.A., Matunis, M.J. & Lima, C.D. Structural basis for E2-mediated SUMO conjugation revealed by a complex between ubiquitin-conjugating enzyme Ubc9 and RanGAP1. *Cell* **108**, 345–356 (2002).
23. Hu, M. *et al.* Crystal structure of a UBP-family deubiquitinating enzyme in isolation and in complex with ubiquitin aldehyde. *Cell* **111**, 1041–1054 (2002).
24. VanDemark, A.P. & Hill, C.P. Structural basis of ubiquitylation. *Curr. Opin. Struct. Biol.* **12**, 822–830 (2002).
25. Verdecia, M.A. *et al.* Conformational flexibility underlies ubiquitin ligation mediated by the WWP1 HECT domain E3 ligase. *Mol. Cell* **11**, 249–259 (2003).
26. Walden, H. *et al.* The structure of the APPBP1–UBA3–NEDD8–ATP complex reveals the basis for selective ubiquitin-like protein activation by an E1. *Mol. Cell* **12**, 1427–1437 (2003).
27. Furukawa, M., Zhang, Y., McCarville, J., Ohta, T. & Xiong, Y. The CUL1 C-terminal sequence and ROC1 are required for efficient nuclear accumulation, NEDD8 modification, and ubiquitin ligase activity of CUL1. *Mol. Cell. Biol.* **20**, 8185–8197 (2000).
28. Walden, H., Podgorski, M.S. & Schulman, B.A. Insights into the ubiquitin transfer cascade from the structure of the E1 for NEDD8. *Nature* **422**, 330–334 (2003).
29. Roussel, M.F., Cleveland, J.L., Shurtleff, S.A. & Sherr, C.J. Myc rescue of a mutant CSF-1 receptor impaired in mitogenic signalling. *Nature* **353**, 361–363 (1991).
30. Roussel, M.F., Theodoras, A.M., Pagano, M. & Sherr, C.J. Rescue of defective mitogenic signaling by D-type cyclins. *Proc. Natl. Acad. Sci. U.S.A.* **92**, 6837–6841 (1995).
31. Roussel, M.F. & Sherr, C.J. Mouse NIH 3T3 cells expressing human colony-stimulating factor 1 (CSF-1) receptors overgrow in serum-free medium containing human CSF-1 as their only growth factor. *Proc. Natl. Acad. Sci. USA* **86**, 7924–7927 (1989).
32. Lake, M.W., Wuebbens, M.M., Rajagopalan, K.V. & Schindelin, H. Mechanism of ubiquitin activation revealed by the structure of a bacterial MoeB–MoaD complex. *Nature* **414**, 325–329 (2001).
33. Endicott, J.A., Noble, M.E. & Tucker, J.A. Cyclin-dependent kinases: inhibition and substrate recognition. *Curr. Opin. Struct. Biol.* **9**, 738–744 (1999).
34. Biondi, R.M. & Nebreda, A.R. Signalling specificity of Ser/Thr protein kinases through docking-site-mediated interactions. *Biochem. J.* **372**, 1–13 (2003).
35. Takeda, D.Y., Wohlschlegel, J.A. & Dutta, A. A bipartite substrate recognition motif for cyclin-dependent kinases. *J. Biol. Chem.* **276**, 1993–1997 (2001).
36. Yashiroda, H. & Tanaka, K. But1 and But2 proteins bind to Uba3, a catalytic subunit of E1 for neddylation, in fission yeast. *Biochem. Biophys. Res. Commun.* **311**, 691–695 (2003).
37. Lyapina, S. *et al.* Promotion of NEDD8-CUL1 conjugate cleavage by COP9 signalosome. *Science* **292**, 1382–1385 (2001).
38. Kolman, C.J., Toth, J. & Gonda, D.K. Identification of a portable determinant of cell cycle function within the carboxyl-terminal domain of the yeast CDC34 (UBC3) ubiquitin conjugating (E2) enzyme. *EMBO J.* **11**, 3081–3090 (1992).
39. Silver, E.T., Gwozd, T.J., Ptak, C., Goebl, M. & Ellison, M.J. A chimeric ubiquitin conjugating enzyme that combines the cell cycle properties of CDC34 (UBC3) and the DNA repair properties of RAD6 (UBC2): implications for the structure, function and evolution of the E2s. *EMBO J.* **11**, 3091–3098 (1992).
40. Haldeman, M.T., Xia, G., Kasperek, E.M. & Pickart, C.M. Structure and function of ubiquitin conjugating enzyme E2-25K: the tail is a core-dependent activity element. *Biochemistry* **36**, 10526–10537 (1997).
41. Morrison, A., Miller, E.J. & Prakash, L. Domain structure and functional analysis of the carboxyl-terminal polyacidic sequence of the RAD6 protein of *Saccharomyces cerevisiae*. *Mol. Cell. Biol.*, **8**, 1179–1185 (1998).
42. Madura, K., Dohmen, R.J. & Varshavsky, A. N-recognin/Ubc2 interactions in the N-end rule pathway. *J. Biol. Chem.* **268**, 12046–12054 (1993).
43. Pan, Z.Q., Kentsis, A., Dias, D.C., Yamoah, K. & Wu, K. Nedd8 on cullin: building an expressway to protein destruction. *Oncogene* **23**, 1985–1997 (2004).
44. Bencsath, K.P., Podgorski, M.S., Pagala, V.R., Slaughter, C.A. & Schulman, B.A. Identification of a multifunctional binding site on Ubc9p required for Smt3p conjugation. *J. Biol. Chem.* **277**, 47938–47945 (2002).
45. Zheng, N. *et al.* Structure of the Cul1–Rbx1–Skp1–F box^{Skp2} SCF ubiquitin ligase complex. *Nature* **416**, 703–709 (2002).
46. Bohnsack, R.N. & Haas, A.L. Conservation in the mechanism of Nedd8 activation by the human AppBp1–Uba3 heterodimer. *J. Biol. Chem.* **278**, 26823–26830 (2003).
47. Hannon, G.J. *et al.* MaRX: an approach to genetics in mammalian cells. *Science* **283**, 1129–1130 (1999).
48. Otwinowski, Z. & Minor, W. Processing of X-ray diffraction data collected in oscillation mode. *Methods Enzymol.* **176**, 307–326 (1997).
49. Holton, J. & Alber, T. Automated protein crystal structure determination using ELVES. *Proc. Natl. Acad. Sci. USA* **101**, 1537–1542 (2004).
50. Brünger, A.T. *et al.* Crystallography & NMR system: a new software suite for macromolecular structure determination. *Acta Crystallogr. D* **54**, 905–921 (1998).
51. Whitby, F.G., Xia, G., Pickart, C.M. & Hill, C.P. Crystal structure of the human ubiquitin-like protein NEDD8 and interactions with ubiquitin pathway enzymes. *J. Biol. Chem.* **273**, 34983–34991 (1998).